Geophysical Research Letters

RESEARCH LETTER
10.1029/2022GL098149

Asymmetries in Circulation Anomalies Related to the Phases of the North Atlantic Oscillation on Synoptic Time Scales

T. Schmith[1], S. M. Olsen[1], S. Yang[1], and J. H. Christensen[1,2,3]

[1]National Centre for Climate Research, Danish Meteorological Institute, Copenhagen, Denmark, [2]Physics of Ice, Climate and Earth, Niels Bohr Institute, University of Copenhagen, Copenhagen, Denmark, [3]NORCE Norwegian Research Centre, Bjerknes Centre for Climate Research, Bergen, Norway

Abstract The North Atlantic Oscillation (NAO) index is often characterized by independent positive and negative NAO events with a characteristic spatial pattern and a typical lifetime of around 1 week. These events are separated by periods of near-neutral NAO conditions. Here, we challenge this view by showing in reanalysis and observed data that the strength and spatial shape of NAO events depends on the NAO index prior to the window of 1 week and this dependency is most pronounced for negative NAO events. The influence is seen in the mean sea level pressure, and in other important features, including blocking frequency and jet stream characteristics, and also in air surface temperature and precipitation in parts of Europe. This new appreciation is important for efforts to improve methods for subseasonal-to-seasonal predictions of NAO.

Plain Language Summary Northern European winters differ. Some are mild and moist with prevailing westerly winds and some are cold and dry, dominated by the Siberian air masses from East. When the Northern European winters are mild, the winter in Greenland is cold, and vice versa. This is the North Atlantic Oscillation (NAO) and its companion, the Europe–Greenland temperature seesaw. They were described in qualitative terms already in the late eighteenth century. Nowadays, the NAO is often described as a series of independent positive or negative events with a duration of around 1 week with intermittent periods of near-neutral conditions and variable duration. The net result of these events determines the NAO strength of the winter. We show that this picture is too simplified because the NAO outside the time horizon of 1 week influences the strength of the individual NAO events. This is most pronounced for the negative events where this influence can both distort and amplify or diminish the pattern of the event. Also the typical temperatures and precipitation patterns associated with NAO are influenced significantly by this effect. One important consequence for our discovery is the improved prospects of doing subseasonal-to-seasonal predictions.

Key Points:

- The daily North Atlantic Oscillation (NAO) index consists of positive and negative events of duration around 1 week separated by periods of near-neutral conditions
- The strength and spatial shape of negative NAO events depends on NAO-index values prior to the event
- Blocking frequencies, jet strength and position, and surface temperature and precipitation have similar dependencies

Supporting Information:

Supporting Information may be found in the online version of this article.

Correspondence to:

T. Schmith,
ts@dmi.dk

Citation:

Schmith, T., Olsen, S. M., Yang, S., & Christensen, J. H. (2022). Asymmetries in circulation anomalies related to the phases of the North Atlantic Oscillation on synoptic time scales. *Geophysical Research Letters*, *49*, e2022GL098149. https://doi.org/10.1029/2022GL098149

Received 31 JAN 2022
Accepted 27 MAY 2022

Author Contributions:

Conceptualization: T. Schmith, S. M. Olsen
Investigation: T. Schmith
Methodology: T. Schmith, S. M. Olsen, S. Yang, J. H. Christensen
Writing – original draft: T. Schmith
Writing – review & editing: S. M. Olsen, S. Yang, J. H. Christensen

1. Introduction

The North Atlantic Oscillation (NAO) is the most important mode of atmospheric variability during winter over Europe and the North Atlantic region on interannual and longer time scales. The NAO is a variability pattern in the mean sea level pressure (MSLP) with centers of action of opposite polarity near Iceland and the Azores, and the NAO index measures the strength of the MSLP gradient between the centers of action. A change in the NAO index is thus a change in the mean strength of the westerlies over the North Atlantic area and a change in the associated advection pattern of air masses. Specifically, a positive (negative) NAO index means above (below) average westerlies. It is also important to remember that the NAO index, despite its name, fluctuates from year to year in a nonoscillatory fashion. For a recent overview of relevant literature, see Stendel et al. (2016).

We can presume that these NAO-related changes in advection patterns influence the prevailing weather of European winters. The literature documents this for European temperatures and precipitation, including extremes of daily temperatures (Kenyon & Hegerl, 2008) and precipitation (Haylock & Goodess, 2004), as well as North Atlantic storm track strength and position, and sea surface temperatures, sea ice occurrence, and other ocean characteristics (Hurrell & Deser, 2010).

The NAO is not confined to the surface but is an almost equivalent barotropic pattern throughout the entire troposphere (e.g., Wanner et al., 2001). The NAO is thus a major dynamical feature of the atmosphere in the region and as such influences and interacts with other dynamical features. Thus, significantly more blocking episodes are observed over the North Atlantic during winters dominated by negative NAO index compared to winters

with positive NAO index (Shabbar et al., 2001). Also the meridional position of the Atlantic jet changes with the phases of the NAO (Woollings et al., 2010).

Besides the NAO mode, the East Atlantic (e.g., Wallace & Gutzler, 1981) and Scandinavian patterns (e.g., Barnston & Livezey, 1987) contribute to the variability in surface weather, etc. described above. They are, however, less dominant modes and are therefore not included in this analysis.

For long, the "state" of the NAO has been regarded as a feature of a given winter. Feldstein (2000) argued that the study of the *daily* NAO index could reveal insight into the processes behind the NAO variability. He noted that empirical orthogonal functions (EOF) analysis of the 300 hPa geopotential height field in daily, monthly, and seasonal time resolution yielded remarkably similar patterns related to NAO and took that as an argument that the fundamental time scale of the NAO was in the order of days. He also estimated the decorrelation time of the daily NAO index to be near 10 days, which we will refer to as the *synoptic time scale*. The NAO therefore consists of positive and negative events lasting around 1 week with intermittent periods of near-neutral conditions. The net number of events combined with their magnitude then defines the NAO index for each winter.

Here, we will demonstrate that this picture is too simplified. Our analysis reveals that the NAO index prior to the time horizon of 1 week has an impact on the strength and spatial pattern of the following NAO events, including the associated circulation features and temperature and precipitation patterns. This is particularly true for negative events. When this influence is significant, we will refer to it as *preconditioning* throughout this paper.

2. Data and Definitions

We analyze daily averages of MSLP over the North Atlantic/European area, supplemented by other fields from the ERA5 reanalysis and E-OBS gridded observation data sets for the period 1950–2020. Details on data and calculation of climatologies and anomalies are in the Supporting Information S1.

2.1. The Daily NAO Index

We calculate the NAO spatial pattern from EOF analysis of the winter (DJF) mean MSLP fields. This pattern explains 49% of the total variability. The winter daily NAO index is the projection of the daily MSLP anomaly field onto the winter NAO spatial pattern. Cosine-latitude weighting is applied in both EOF analysis and the projection. The index is normalized to have unit variance.

2.2. NAO Events

We identify NAO^+ and NAO^- peak days during winter (DJF) as local maxima and minima, respectively, in the daily NAO index which in absolute value exceeds one standard deviation of the daily NAO index. When two (or more) peaks are detected within a 12-day time window, only the peak with the largest amplitude is kept; the others are ignored. Thus, neighboring peaks (positive or negative) are separated by at least 12 days. This is more than the decorrelation time of the daily NAO (see Section 1) and therefore ensures that neighboring peaks are approximately statistically independent. An event is defined as the peak day and the three neighboring days before and after; in all 7 days. For illustration, we show the daily NAO index and identified NAO^+ and NAO^- events for selected years with high, neutral, and negative winter (DJF) NAO index in Figure S1 in Supporting Information S1. In total, we detect 139 NAO^+ events and 99 NAO^- events for the whole analysis period. We also show in Figure S2 in Supporting Information S1 the expected positive(negative) correlation between the winter mean NAO index and the number of NAO^+ (NAO^-) events.

2.3. NAO Precursor

We seek to understand how the MSLP anomaly pattern corresponding to the identified NAO events depends on the NAO index further back in time beyond the synoptic time scale of around 10 days. We therefore define the NAO precursor value (NAO_{pre}) for a given NAO event as the averaged daily NAO index over day 10 to day 30 prior to the peak day of the NAO event. The 10-day limit is chosen as being outside the synoptic window. The 30-day limit allows the precursor to be calculated for all winter days, including 1 December, and still staying within November which could be regarded as belonging to the (extended) winter. In Figure S3 in Supporting

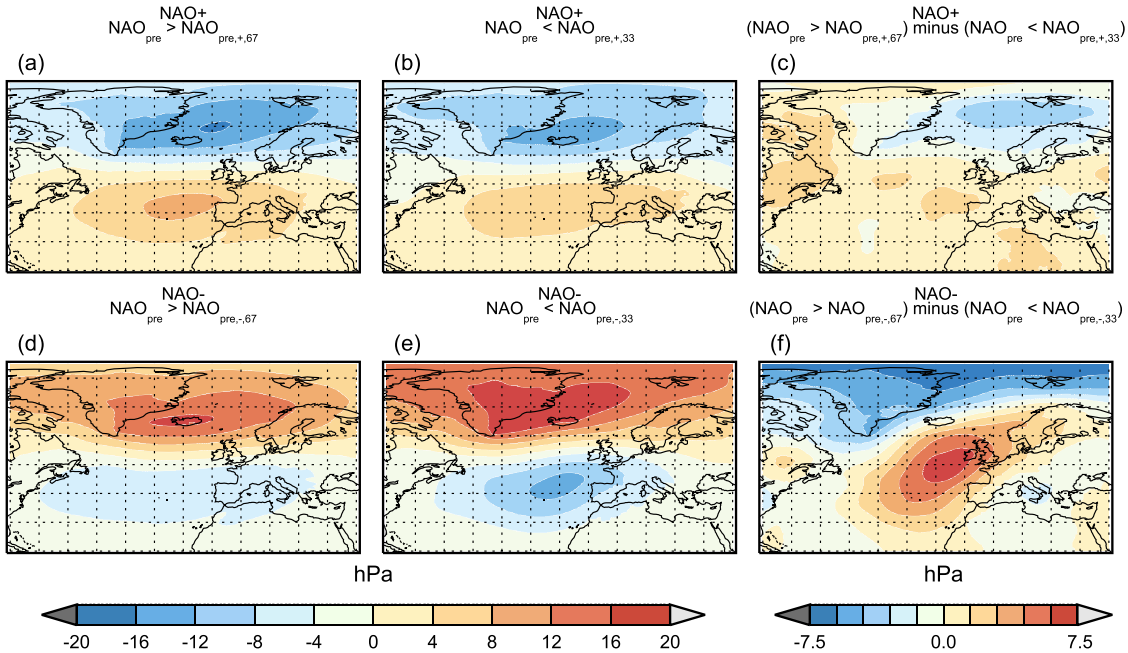

Figure 1. Composite mean sea level pressure (MSLP) anomalies for (a, b) NAO$^+$ and (d, e) NAO$^-$ events, combined with (a, d) $NAO_{pre} > NAO_{pre,x,67}$ and (b, e) $NAO_{pre} < NAO_{pre,\,x,33}$ (x is either "+" or "−"). (c, f) The corresponding composite differences for NAO$^+$ and NAO$^-$ events, respectively.

Information S1, we show the observed frequency of NAO_{pre} for NAO$^+$ and NAO$^-$ events separately. The two frequency curves are shifted toward positive and negative values of NAO_{pre}, respectively. This is a first hint that NAO_{pre} impacts the details of the two types of events. This will be detailed in the analysis below.

3. Analysis and Results

3.1. NAO Events and Their Signal in the MSLP Field

We show in Figure S4 in Supporting Information S1, MSLP composites of NAO$^+$ and NAO$^-$ events and their difference. Both these MSLP composites resemble their well-known equivalent obtained from winter mean data. Therefore, the composite difference has negative anomalies near Iceland and positive near Azores. The maximum pressure difference between Iceland and Azores in this composite difference is more than 50 hPa and therefore around 6 times larger than corresponding mean pressure difference of around 8 hPa in the winter mean NAO pattern (Hurrell et al., 2003).

We investigate the dependency on the NAO precursor for NAO$^+$ (Figures 1a and 1b) and NAO$^-$ (Figures 1d and 1e) events separately in order to account for any asymmetries. In each case, we make the composite anomaly maps of MSLP corresponding to the upper and lower terciles of NAO_{pre}. To be more specific, we make composites corresponding to $NAO_{pre} > NAO_{pre,+,67}$, where $NAO_{pre,+,67}$ is the 67th percentile of NAO_{pre} for NAO$^+$ events, and similarly for $NAO_{pre} < NAO_{pre,+,33}$. Finally, the difference of these two MSLP anomaly composites is calculated (Figures 1c and 1f). The same procedure is used for NAO$^-$ events.

The gross features of the MSLP composite patterns corresponding to both NAO$^+$ and NAO$^-$ events are unchanged regardless of NAO_{pre}. However, the composite difference maps in Figures 1c and 1f reveal important differences between the NAO$^+$ and NAO$^-$ composites. The effect of NAO_{pre} is largest for NAO$^-$ events (Figure 1f), where the largest induced pressure difference is around 14 hPa between extrema near British Isles and over Greenland. For NAO$^-$ events, the variability related to NAO_{pre} is thus a notable fraction of almost 30% of the difference of around 50 hPa between NAO$^+$ and NAO$^-$ events seen in Figure S4 in Supporting Information S1. However, since the two patterns are not spatially aligned, the NAO_{pre}-related variability both reinforces/weakens the NAO$^-$ composite and changes its shape. For NAO$^+$ events, the pattern corresponding to NAO_{pre}-related variability shown in Figure 1c is more unstructured and the pressure differences are smaller. Therefore, the preconditioning is stronger and more pronounced for NAO$^-$ events than for NAO$^+$ events.

We evaluated statistically the probability for the patterns in Figures 1c and 1f to occur by chance. This was done by comparing the patterns with the background distribution function obtained using bootstrapping. Details are described in Supporting Information S1 and results are in Figure S5 in Supporting Information S1. This statistical analysis yields that patterns are near the 50th percentile for NAO^+ events (Figure 1c), but close to the 95th percentile for NAO^- events (Figure 1f). Thus, the preconditioning is statistically significant near the 5% level in the NAO^- case, which virtually excludes that we are just highlighting interannual variability. In the NAO^+ case, there is a large risk that the identified preconditioning is a finite-sampling artifact and not a true NAO_{pre}-related dependency.

The asymmetry we have identified may have wider imprints outside the region of interest to the current study. Therefore, we also provide global versions of the above composites in Figure S6 in Supporting Information S1, noting that a detailed analyses of these are outside the scope of the present work.

3.2. Atmospheric Blocking

We describe atmospheric blockings by the longitudinal blocking index by Tibaldi and Molteni (1990) and by the two-dimensional absolute geopotential height blocking index by Scherrer et al. (2006), henceforth the TM90-index and the S06-index, respectively. Both indices are calculated from the daily mean 500 hPa geopotential height. Details on calculating the two blocking indices are in Supporting Information S1.

Blocking frequencies for NAO^+ and NAO^- events are shown in Figure S7a in Supporting Information S1. For the TM90-index (Figure S7a in Supporting Information S1), the climatological winter (DJF) mean has a maximum near 5°E. There are clear differences with nonoverlapping confidence intervals in the occurrence of blockings between NAO^+ and NAO^- events. For NAO^+ events, the maximum frequency is near 20°E with negligible blocking frequency west of 20°W, while for NAO^- events there is a pronounced occurrence of blockings between 20°W and 40°W. The patterns of blocking occurrence during NAO^+ and NAO^- events are also very different in the S06-index. Blockings appear mostly in the southeastern of North Atlantic from west of Iberia stretching to Germany during NAO^+ (Figure S7b in Supporting Information S1). During NAO^- events, enhanced blocking frequencies are in an extensive band stretching from southern Greenland to mid-Scandinavia (Figure S7c in Supporting Information S1). The linkage between NAO and blocking activities has been found in several other studies (e.g., Croci-Maspoli et al., 2007).

We also investigate the dependency on the NAO_{pre} of blocking frequencies for NAO^+ and NAO^- events separately. The qualitative behavior of the blocking frequency and location associated with the NAO^+ events appear quite independent of the sign of NAO_{pre} with negligible blockings over the Atlantic in the TM90-index (Figure 2a), and the corresponding S06-index of the blocking frequency (Figures 2b and 2d) is quite similar to that of the NAO^+ mean (Figure S7b in Supporting Information S1) with the band of enhanced blocking frequency changing its shape a bit according to whether NAO_{pre} is positive or negative. These changes, most clearly seen in the difference plot (Figure 2f), are mostly insignificant on the 5% level, with only a tiny significant area over the English Channel.

For NAO^- events, the dependency on NAO_{pre} is very different and more significant. In the TM-90 index (Figure 2a), maximum blocking frequencies are between 0°W and 20°W for $NAO_{pre} > NAO_{pre,-,67}$, while they are between 20°W and 40°W for $NAO_{pre} < NAO_{pre,-,33}$. However, this difference is within the confidence limits, except west of 60°W. However, the TM90-index is a latitude-integrated index and therefore things may look different in the S06-index. In the S06-index, the area with large blocking frequency shifts toward eastern North Atlantic and Scandinavia for $NAO_{pre} > NAO_{pre,-,67}$ (Figure 2c) in comparison with the climatology (Figure S7c in Supporting Information S1), demonstrating a clear increase of the occurrence of Scandinavian blockings. For $NAO_{pre} < NAO_{pre,-,33}$, the S06-index shifts westwards with an increase of Greenland blockings (Figure 2e). Differences are seen clearly in Figure 2g with a large area of significant changes over Scandinavia and an area with significant changes of the opposite sign near Southern Baffin Island.

In summary, we find a significant preconditioning in the spatial distribution of blocking frequencies for NAO^- events, while this is not the case for NAO^+ events. This is in line with our earlier findings.

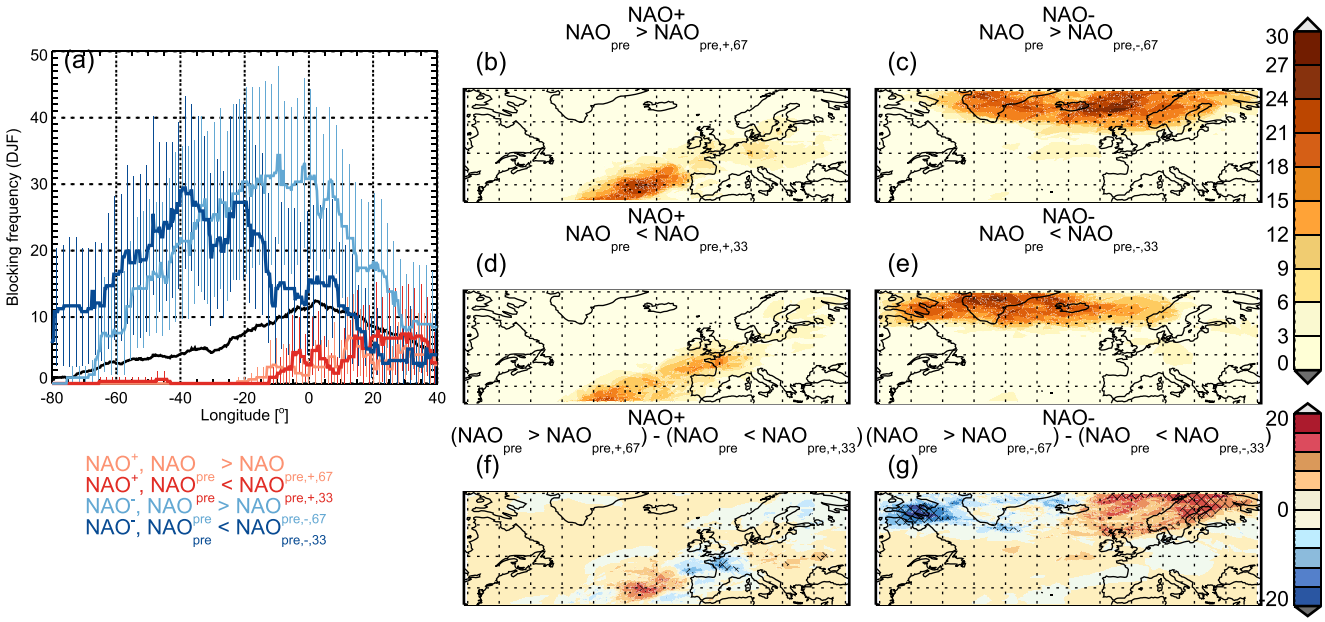

Figure 2. DJF mean blocking frequency (percentage of days with blocking). (a) TM90 blocking index. Red (blue) lines refer to NAO^+ (NAO^-) events. Light (dark) hues refer to $NAO_{pre} > NAO_{pre,x,67}$ ($NAO_{pre} < NAO_{pre,x,33}$; x is either "+" or "−"). Vertical, colored lines show 95% confidence intervals. Black line is the climatology. (b–e) S06 blocking index composites: NAO^+ (b, d) and NAO− (c, e) events, combined with (b, c) $NAO_{pre} > NAO_{pre,x,67}$ and (d, e) $NAO_{pre} < NAO_{pre,x,33}$. (f, g) Composite differences between $NAO_{pre} > NAO_{pre,x,67}$ and $NAO_{pre} < NAO_{pre,x,33}$ for NAO^+ and NAO^- events, respectively. Differences significant on the 5% level from resampling with replacement are cross-hatched.

3.3. Jet Stream Speed and Latitude

We characterize the speed and latitude of the tropospheric westerly jet stream using a modified version of the method in Woollings et al. (2010). See Supporting Information S1 for details.

Figure S8 in Supporting Information S1 shows probability distribution of jet speed and jet latitude index for NAO^+ and NAO^- events. The distribution of the jet stream speed exhibits a clear shift toward stronger (weaker) and more northern (southern) latitudes for NAO^+ (NAO^-) events, and these shifts are significant on a very high level according to a Kolmogorov–Smirnov test.

The effect of NAO_{pre} on jet strength and position is illustrated by the probability densities shown in Figure 3. For NAO^+ events, the dependencies on NAO_{pre} are small and not very significant (large p-values). For NAO^- events, the jet stream speeds are slightly shifted for higher $NAO_{pre} < NAO_{pre,-,33}$ compared to $NAO_{pre} > NAO_{pre,-,67}$ but this is not very significant. The jet stream for $NAO_{pre} < NAO_{pre,-,33}$ also generally shifts to a more southerly position compared $NAO_{pre} > NAO_{pre,-,67}$, and this is highly significant. This is in accord with the large and significant signal found in Figure 1f, and consistent with the higher Greenland blocking frequency seen in Section 3.2 and Figure 2.

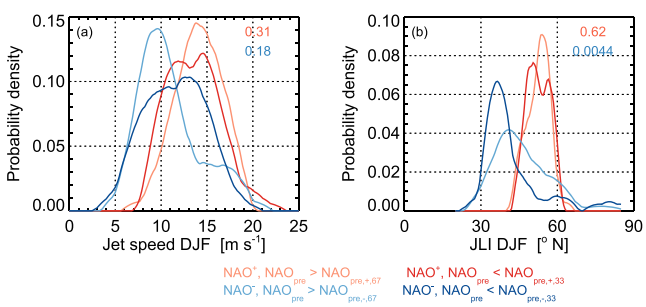

Figure 3. Probability densities of (a) jet stream speed and (b) jet latitude index. Red lines are for NAO^+ events, blue lines are for NAO^- events. Light (dark) hues refer to $NAO_{pre} > NAO_{pre,x,67}$ ($NAO_{pre} < NAO_{pre,x,33}$; x is either "+" or "−"). Blue and red numbers are p-values of a Kolmogorov–Smirnov test of the distributions for $NAO_{pre} > NAO_{pre,x,67}$ and $NAO_{pre} < NAO_{pre,x,33}$ being different, for NAO^+ and NAO^- events, respectively.

3.4. Surface Weather

Variability in European weather conditions is linked to the state of the NAO. Therefore, it is also of interest to investigate its dependency on NAO_{pre} for both types of NAO events.

3.4.1. Surface Air Temperature

Surface air temperature (SAT) varies between NAO^+ and NAO^- events in many parts of Europe. This is seen in the composite maps of Figure S9 in Supporting Information S1. Largest signals in (c) the difference pattern are

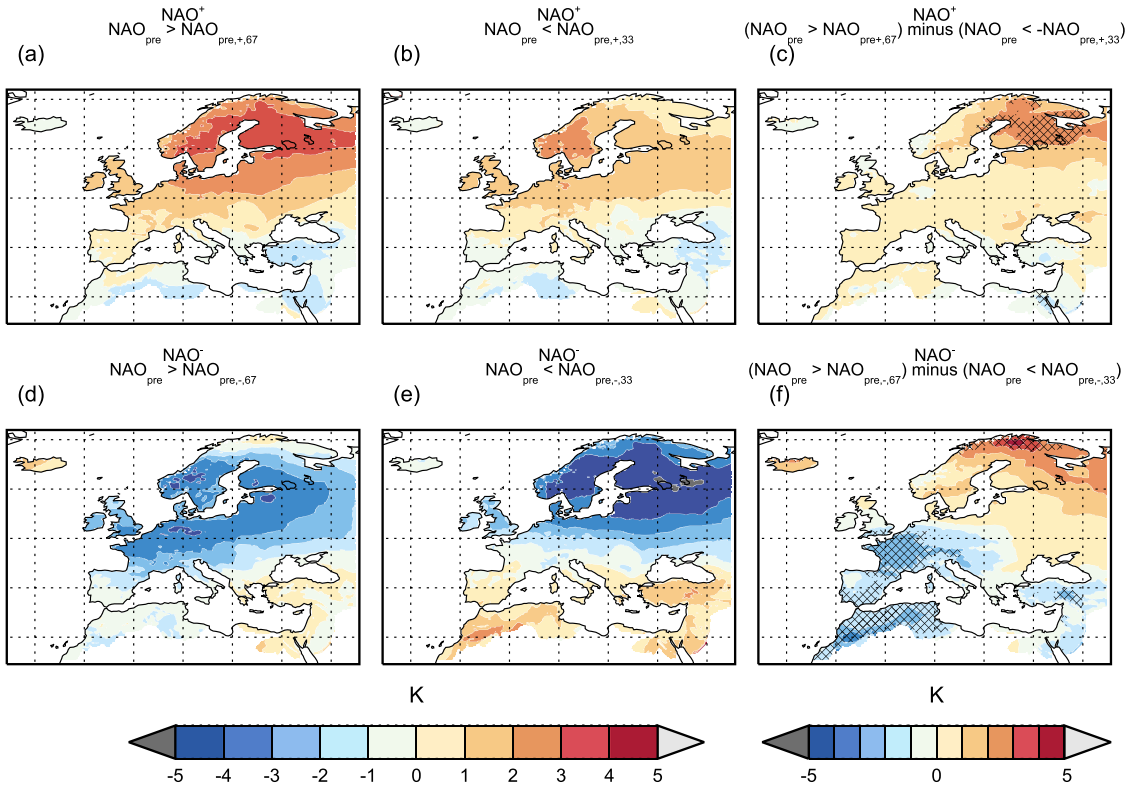

Figure 4. Composite surface air temperature (SAT) anomalies for (a, b) NAO$^+$ and (d, e) NAO$^-$ events, combined with (a, d) $NAO_{pre} > NAO_{pre,x,67}$ and (b, e) $NAO_{pre} < NAO_{pre,x,33}$ (x is either "+" or "−"). (c, f) Composite differences between $NAO_{pre} > NAO_{pre,x,67}$ and $NAO_{pre} < NAO_{pre,x,33}$ for NAO$^+$ and NAO$^-$ events, respectively. Differences significant on the 5% level from resampling with replacement are cross-hatched.

over Scandinavia up to around 7 K, and a smaller signal of opposite polarity around the Mediterranean up to around 3 K.

Figure 4 shows composites of European SAT for NAO$^+$ and NAO$^-$ events in combination with $NAO_{pre} > NAO_{pre,x,67}$ and $NAO_{pre} < NAO_{pre,x,33}$. For NAO$^+$ events, the well-known pattern of positive SAT anomalies is largely reproduced, but the NAO_{pre} seems to play a role in shaping the finer details. Thus, $NAO_{pre} > NAO_{pre,+,67}$ gives a strengthened positive anomaly pattern, while $NAO_{pre} < NAO_{pre,+,33}$ gives a weakened positive SAT anomaly pattern. The difference between these two is positive over whole Europe and largest, up to around 3 K, over the Scandinavia and significant on the 5% level.

For NAO$^-$ events, there is a strong negative SAT anomaly pattern, when $NAO_{pre} < NAO_{pre,-,33}$ while for $NAO_{pre} > NAO_{pre,-,67}$ the SAT anomaly pattern exhibits weaker negative SAT anomalies over large parts of Northern Europe and even positive anomalies, which are significant at the 5% level, over northern Scandinavian Peninsula and Iceland. We also find relatively large and statistically significant differences of the opposite polarity over France and Middle East.

3.4.2. Precipitation

Also for precipitation, there is some effect of preconditioning. For NAO$^+$ events, there are positive anomalies in Northern Europe which are up to around 2.5 mm day^{-1} in Western Norway and Scotland. But they generally seem larger for $NAO_{pre} > NAO_{pre,+,67}$ (Figure S11a in Supporting Information S1), compared to $NAO_{pre} < NAO_{pre,+,33}$ (Figure S11b in Supporting Information S1), as is easily seen in the difference plot (Figure S11c in Supporting Information S1), where differences are also up to 2.5 mm day^{-1}. These differences are generally not found to be significant on the 5% level.

For NAO$^-$ events (Figure S11d–S11f in Supporting Information S1), we see a different dependence on NAO_{pre}. Differences related to positive and negative NAO_{pre}, respectively, are generally small in Northern Europe, while

the largest and also significant differences occur over the Iberian Peninsula. A small area of significant differences are also found over Eastern Europe although the differences themselves are relatively small.

4. Discussion

4.1. Relation to Other Work

Some of the findings in this study are reflected in previous studies. Kushnir et al. (2006) found a decay time scale around 10 days in the autocorrelation function of daily NAO index, but in addition identified a secondary "shoulder" near 2–5 weeks Keeley et al. (2009), however, demonstrated that interannual variability is a source of uncertainty for this type of study. Also Rennert and Wallace (2009) analyzed daily NAO variability and confirmed the decorrelation time scale of 10 days but also found "shoulders" beyond that time scale. Finally, Önskog et al. (2018) confirmed the decorrelation time scale of around 10 days but in addition found long-range dependence in the daily NAO index. These studies do not, however, analyze NAO^+ and NAO^- events separately, and therefore they do not find the important differences in preconditioning between NAO^+ and NAO^- events, as we do here.

The growth and decay of NAO events are investigated in Benedict et al. (2004), Feldstein (2003), and Franzke et al. (2004). They find that upper-tropospheric Rossby wave breaking plays an important role in the growth of the NAO events. They additionally point out that the wave breaking takes place both locally over the North Atlantic and remotely over the North American west coast for the NAO^+ events, while takes place solely locally over the North Atlantic for the NAO^- events. We suggest that this more local character of the NAO^- events is related to the prominent preconditioning we find, although a rigorous analysis is needed to settle this.

We also note that recent studies showed that the succession of blockings and its associated upper-level Rossby wave breaking events over the North Atlantic may give rise to low-frequency variability of the NAO (Woollings et al., 2008). In particular, the Greenland blockings are strongly coupled to the NAO and can modulate the NAO patterns (Davini et al., 2012). Our results suggest that persistent NAO^- events (implying $NAO_{pre} < NAO_{pre,-,33}$) may also precondition the large-scale circulation that favors the occurrence of blockings. Finally, Hannachi et al. (2012) find persistence beyond the synoptic time scale for the southerly position of the jet stream, corresponding to NAO^- events.

Besides the extratropical mechanisms based on Rossby wave breaking, there could be sources of tropical origin for the observed variability. These include ENSO (Toniazzo & Scaife, 2006), the Julian–Madden oscillation (Cassou, 2008), and the quasi-biennial oscillation (Andrews et al., 2019). These suggestions invite to more comprehensive follow-up studies using observations and dedicated modeling.

4.2. Sampling Uncertainties

The most severe limitation in observational climate studies is often the length of the observational record of 100–150 years for ground observations, and around 75 years for upper-air observations. Combined with the presence of decadal-scale variability, this means that sampling uncertainty is the most important source of uncertainty. This means that the patterns shown in Figure 1 are somewhat dependent of the exact time period considered and are only approximately equal to the true pattern, which we could only estimate if we have had a timely unlimited record available.

Of particular interest is to know whether the difference patterns in Figures 1c and 1f are identically zero, since that would mean no dependence on NAO_{pre}. This cannot be categorically verified/falsified but probabilities can be obtained, and this is exactly the purpose of the bootstrap-procedure described in Supporting Information S1.

With ongoing and future anthropogenic climate change and the need for attribution of these, it is generally important to separate internal variability from any forced signal. This is particularly important in the North Atlantic–European region, since the magnitude and in some areas even the sign of projected European temperature and precipitation changes could vary with the phase of the NAO (Deser et al., 2017). Therefore, emerging climate change signals in temperature and precipitation are delayed, compared to a hypothetical situation without NAO-related variability (e.g., Kjellström et al., 2013).

4.3. Subseasonal-to-Seasonal Predictions

Knowing the temporal correlations of the daily NAO index beyond the synoptic time scale could contribute to exploring the possibilities for subseasonal-to-seasonal (S2S) predictions in the North Atlantic area and Europe. There are ongoing international efforts to advance the capability of S2S predictions (Lang et al., 2020; Mariotti et al., 2018, 2020). Present S2S predictions of the NAO are generally not without problems (Albers & Newman, 2021; Smith et al., 2016), most likely related to the signal-to-noise paradox (Dunstone et al., 2019).

The question of preconditioning outside the synoptic time scale is important for assessing the possibilities of seasonal prediction of the NAO. Seasonal predictability of the NAO has been heavily discussed in recent years based on time series analysis (Domeisen et al., 2018), hybrid model-empirical methods (Dobrynin et al., 2018). The paradigm of independent NAO events put forward in the Section 1 questions the possibility of predicting the NAO beyond a week or so. Opposed to that, our study supports such predictions being possible, at least for NAO^- events.

5. Summary

We analyze reanalyses and observations and find that the notion of independent positive and negative NAO events with intermittent stages of near-neutral conditions is not complete. We find that the MSLP patterns and other circulation conditions associated with NAO^+ and NAO^- events are influenced by the NAO phase prior to these and hence outside the synoptic time scale of around 10 days—what we call the NAO precursor and define as the average NAO index over days 10–30 before the actual event. For NAO^- events, we find a quite large and statistically significant dependence of the NAO precursor in the MSLP signal, which we identify as a significant preconditioning. Related significant changes are seen in atmospheric blocking frequencies and jet stream characteristics as well as in European surface temperature and precipitation anomaly patterns. For the NAO^+ events, in contrary, the preconditioning effect is smaller and is not found to be statistically significant.

Conflict of Interest

The authors declare no conflicts of interest relevant to this study.

Data Availability Statement

We acknowledge the use of the ERA5 reanalysis (https://doi.org/10.24381/cds.bd0915c6) and the E-OBS data set (https://doi.org/10.24381/cds.151d3ec6). Both data sets can be downloaded from the Copernicus Climate Change Services (https://climate.copernicus.eu).

Acknowledgments
This work was supported by the Blue-Action project (European Union's Horizon 2020 research and innovation program, grant 727852). Part of the funding was provided by the Danish State through the Danish Climate Atlas. Jens H. Christensen received funding from Independent Research Fond Denmark grant number 0217-00244B.

References

Albers, J. R., & Newman, M. (2021). Subseasonal predictability of the North Atlantic Oscillation. *Environmental Research Letters*, *16*(4), 044024. https://doi.org/10.1088/1748-9326/abe781

Andrews, M. B., Knight, J. R., Scaife, A. A., Lu, Y., Wu, T., Gray, L. J., & Schenzinger, V. (2019). Observed and simulated teleconnections between the stratospheric quasi-biennial oscillation and Northern Hemisphere winter atmospheric circulation. *Journal of Geophysical Research: Atmospheres*, *124*, 1219–1232. https://doi.org/10.1029/2018JD029368

Barnston, A. G., & Livezey, R. E. (1987). Classification, seasonality and persistence of low-frequency atmospheric circulation patterns. *Monthly Weather Review*, *115*(6), 1083–1126. https://doi.org/10.1175/1520-0493(1987)115<1083:CSAPOL>2.0.CO;2

Benedict, J. J., Lee, S., & Feldstein, S. B. (2004). Synoptic view of the North Atlantic Oscillation. *Journal of the Atmospheric Sciences*, *61*, 24. https://doi.org/10.1175/1520-0469(2004)061<0121:SVOTNA>2.0.CO;2

Cassou, C. (2008). Intraseasonal interaction between the Madden–Julian Oscillation and the North Atlantic Oscillation. *Nature*, *455*(7212), 523–527. https://doi.org/10.1038/nature07286

Croci-Maspoli, M., Schwierz, C., & Davies, H. C. (2007). Atmospheric blocking: Space–time links to the NAO and PNA. *Climate Dynamics*, *29*(7–8), 713–725. https://doi.org/10.1007/s00382-007-0259-4

Davini, P., Cagnazzo, C., Neale, R., & Tribbia, J. (2012). Coupling between Greenland blocking and the North Atlantic Oscillation pattern. *Geophysical Research Letters*, *39*, L14701. https://doi.org/10.1029/2012GL052315

Deser, C., Hurrell, J. W., & Phillips, A. S. (2017). The role of the North Atlantic Oscillation in European climate projections. *Climate Dynamics*, *49*(9–10), 3141–3157. https://doi.org/10.1007/s00382-016-3502-z

Dobrynin, M., Domeisen, D. I. V., Müller, W. A., Bell, L., Brune, S., Bunzel, F., et al. (2018). Improved teleconnection-based dynamical seasonal predictions of boreal winter. *Geophysical Research Letters*, *45*, 3605–3614. https://doi.org/10.1002/2018GL077209

Domeisen, D. I. V., Badin, G., & Koszalka, I. M. (2018). How predictable are the Arctic and North Atlantic Oscillations? Exploring the variability and predictability of the Northern Hemisphere. *Journal of Climate*, *31*(3), 997–1014. https://doi.org/10.1175/JCLI-D-17-0226.1

Dunstone, N., Smith, D., Hardiman, S., Eade, R., Gordon, M., Hermanson, L., et al. (2019). Skilful real-time seasonal forecasts of the dry Northern European summer 2018. *Geophysical Research Letters*, *46*, 12368–12376. https://doi.org/10.1029/2019GL084659

Feldstein, S. B. (2000). The timescale, power spectra, and climate noise properties of teleconnection patterns. *Journal of Climate*, *13*(24), 4430–4440. https://doi.org/10.1175/1520-0442(2000)013<4430:TTPSAC>2.0.CO;2

Feldstein, S. B. (2003). The dynamics of NAO teleconnection pattern growth and decay. *Quarterly Journal of the Royal Meteorological Society*, *129*(589), 901–924. https://doi.org/10.1256/qj.02.76

Franzke, C., Lee, S., & Feldstein, S. B. (2004). Is the North Atlantic Oscillation a breaking wave? *Journal of the Atmospheric Sciences*, *61*(2), 145–160. https://doi.org/10.1175/1520-0469(2004)061<0145:ITNAOA>2.0.CO;2

Hannachi, A., Woollings, T., & Fraedrich, K. (2012). The North Atlantic jet stream: A look at preferred positions, paths and transitions: The North Atlantic jet stream preferred positions. *Quarterly Journal of the Royal Meteorological Society*, *138*(665), 862–877. https://doi.org/10.1002/qj.959

Haylock, M. R., & Goodess, C. M. (2004). Interannual variability of European extreme winter rainfall and links with mean large-scale circulation. *International Journal of Climatology*, *24*(6), 759–776. https://doi.org/10.1002/joc.1033

Hurrell, J. W., & Deser, C. (2010). North Atlantic climate variability: The role of the North Atlantic Oscillation. *Journal of Marine Systems*, *79*(3), 231–244. https://doi.org/10.1016/j.jmarsys.2009.11.002

Hurrell, J. W., Kushnir, Y., Ottersen, G., & Visbeck, M. (2003). An overview of the North Atlantic Oscillation. In *The North Atlantic Oscillation: Climatic significance and environmental impact* (pp. 1–35). Washington, DC: American Geophysical Union. https://doi.org/10.1029/134GM01

Keeley, S. P. E., Sutton, R. T., & Shaffrey, L. C. (2009). Does the North Atlantic Oscillation show unusual persistence on intraseasonal timescales? *Geophysical Research Letters*, *36*, L22706. https://doi.org/10.1029/2009GL040367

Kenyon, J., & Hegerl, G. C. (2008). Influence of modes of climate variability on global temperature extremes. *Journal of Climate*, *21*(15), 3872–3889. https://doi.org/10.1175/2008JCLI2125.1

Kjellström, E., Thejll, P., Rummukainen, M., Christensen, J. H., Boberg, F., Christensen, O. B., & Fox Maule, C. (2013). Emerging regional climate change signals for Europe under varying large-scale circulation conditions. *Climate Research*, *56*(2), 103–119. https://doi.org/10.3354/cr01146

Kushnir, Y., Robinson, W. A., Chang, P., & Robertson, A. W. (2006). The physical basis for predicting Atlantic sector seasonal-to-interannual climate variability. *Journal of Climate*, *19*(23), 5949–5970. https://doi.org/10.1175/JCLI3943.1

Lang, A. L., Pegion, K., & Barnes, E. A. (2020). Introduction to special collection: "Bridging weather and climate: Subseasonal-to-Seasonal (S2S) prediction". *Journal of Geophysical Research: Atmospheres*, *125*, e2019JD031833. https://doi.org/10.1029/2019JD031833

Mariotti, A., Baggett, C., Barnes, E. A., Becker, E., Butler, A., Collins, D. C., et al. (2020). Windows of opportunity for skillful forecasts subseasonal to seasonal and beyond. *Bulletin of the American Meteorological Society*, *101*(5), E608–E625. https://doi.org/10.1175/BAMS-D-18-0326.1

Mariotti, A., Ruti, P. M., & Rixen, M. (2018). Progress in subseasonal to seasonal prediction through a joint weather and climate community effort. *Npj Climate and Atmospheric Science*, *1*(1), 4. https://doi.org/10.1038/s41612-018-0014-z

Önskog, T., Franzke, C. L. E., & Hannachi, A. (2018). Predictability and non-Gaussian characteristics of the North Atlantic Oscillation. *Journal of Climate*, *31*(2), 537–554. https://doi.org/10.1175/JCLI-D-17-0101.1

Rennert, K. J., & Wallace, J. M. (2009). Cross-frequency coupling, skewness, and blocking in the Northern Hemisphere winter circulation. *Journal of Climate*, *22*(21), 5650–5666. https://doi.org/10.1175/2009JCLI2669.1

Scherrer, S. C., Croci-Maspoli, M., Schwierz, C., & Appenzeller, C. (2006). Two-dimensional indices of atmospheric blocking and their statistical relationship with winter climate patterns in the Euro-Atlantic region. *International Journal of Climatology*, *26*(2), 233–249. https://doi.org/10.1002/joc.1250

Shabbar, A., Huang, J., & Higuchi, K. (2001). The relationship between the wintertime North Atlantic Oscillation and blocking episodes in the north Atlantic. *International Journal of Climatology*, *21*(3), 355–369. https://doi.org/10.1002/joc.612

Smith, D. M., Scaife, A. A., Eade, R., & Knight, J. R. (2016). Seasonal to decadal prediction of the winter North Atlantic Oscillation: Emerging capability and future prospects: Seasonal to decadal prediction of the NAO. *Quarterly Journal of the Royal Meteorological Society*, *142*(695), 611–617. https://doi.org/10.1002/qj.2479

Stendel, M., van den Besselaar, E., Hannachi, A., Kent, E. C., Lefebvre, C., Schenk, F., et al. (2016). Recent change—Atmosphere. In M. Quante & F. Colijn (Eds.), *North Sea region climate change assessment* (pp. 55–84). Cham: Springer International Publishing. https://doi.org/10.1007/978-3-319-39745-0_2

Tibaldi, S., & Molteni, F. (1990). On the operational predictability of blocking. *Tellus A*, *42*(3), 343–365. https://doi.org/10.1034/j.1600-0870.1990.t01-2-00003.x

Toniazzo, T., & Scaife, A. A. (2006). The influence of ENSO on winter North Atlantic climate. *Geophysical Research Letters*, *33*, L24704. https://doi.org/10.1029/2006GL027881

Wallace, J. M., & Gutzler, D. S. (1981). Teleconnections in the geopotential height field during the Northern Hemisphere winter. *Monthly Weather Review*, *109*(4), 784–812. https://doi.org/10.1175/1520-0493(1981)109<0784:TITGHF>2.0.CO;2

Wanner, H., Brönnimann, S., Casty, C., Gyalistras, D., Luterbacher, J., Schmutz, C., et al. (2001). North Atlantic Oscillation—Concepts and studies. *Surveys in Geophysics*, *22*(4), 321–381. https://doi.org/10.1023/a:1014217317898

Woollings, T., Hannachi, A., & Hoskins, B. (2010). Variability of the North Atlantic eddy-driven jet stream. *Quarterly Journal of the Royal Meteorological Society*, *136*(649), 856–868. https://doi.org/10.1002/qj.625

Woollings, T., Hoskins, B., Blackburn, M., & Berrisford, P. (2008). A new Rossby wave–breaking interpretation of the North Atlantic Oscillation. *Journal of the Atmospheric Sciences*, *65*(2), 609–626. https://doi.org/10.1175/2007JAS2347.1

References From the Supporting Information

Cornes, R. C., van der Schrier, G., van den Besselaar, E. J. M., & Jones, P. D. (2018). An ensemble version of the E-OBS temperature and precipitation data sets. *Journal of Geophysical Research: Atmospheres*, *123*, 9391–9409. https://doi.org/10.1029/2017JD028200

Hersbach, H., Bell, B., Berrisford, P., Hirahara, S., Horányi, A., Muñoz-Sabater, J., et al. (2020). The ERA5 global reanalysis. *Quarterly Journal of the Royal Meteorological Society*, *146*, 1999–2049. https://doi.org/10.1002/qj.3803

Jung, T., & Leutbecher, M. (2008). Scale-dependent verification of ensemble forecasts. *Quarterly Journal of the Royal Meteorological Society*, *134*, 973–984. https://doi.org/10.1002/qj.255

North, G. R., Bell, T. L., Cahalan, R. F., & Moeng, F. J. (1982). Sampling errors in the estimation of empirical orthogonal functions. *Monthly Weather Review*, *110*, 699–706.

von Storch, H., & Zwiers, F. W. (1999). *Statistical analysis in climate research*. West Nyack, NY: Cambridge University Press.

Woollings, T., Hannachi, A., & Hoskins, B. (2010). Variability of the North Atlantic eddy-driven jet stream. *Quarterly Journal of the Royal Meteorological Society*, *136*, 856–868. https://doi.org/10.1002/qj.625